OMTO, Volume *23*

Supplemental information

Mycobacterium tuberculosis Rv3628 is an effective adjuvant via activation of dendritic cells for cancer immunotherapy

Juan Wu, Heng Yang, Jin-chuan Xu, Zhidong Hu, Wen-fei Gu, Zhen-yan Chen, Jing-xian Xia, Douglas B. Lowrie, Shui-Hua Lu, and Xiao-Yong Fan

Supplementary Figures

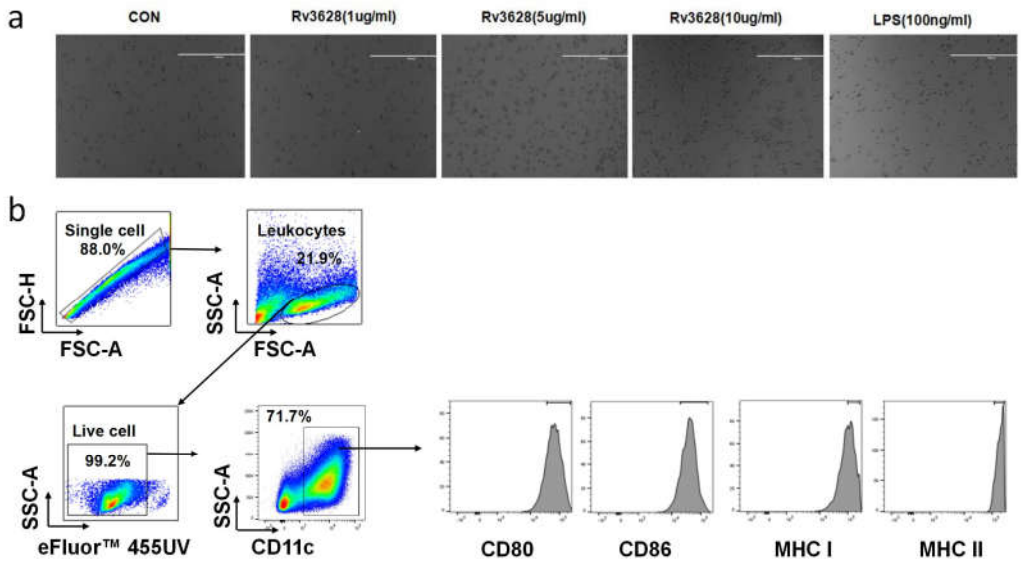

Figure S1. Morphological changes of BMDCs and flow cytometry analysis of BMDCs after treatment with Rv3628. BMDCs were treated with 1, 5, 10 μg/ml Rv3628 or with 100 ng/ml LPS for 24 h. (**a**) Morphological changes of BMDCs. (**b**) Representative graphs showing the gating strategy for analysis of BMDCs.

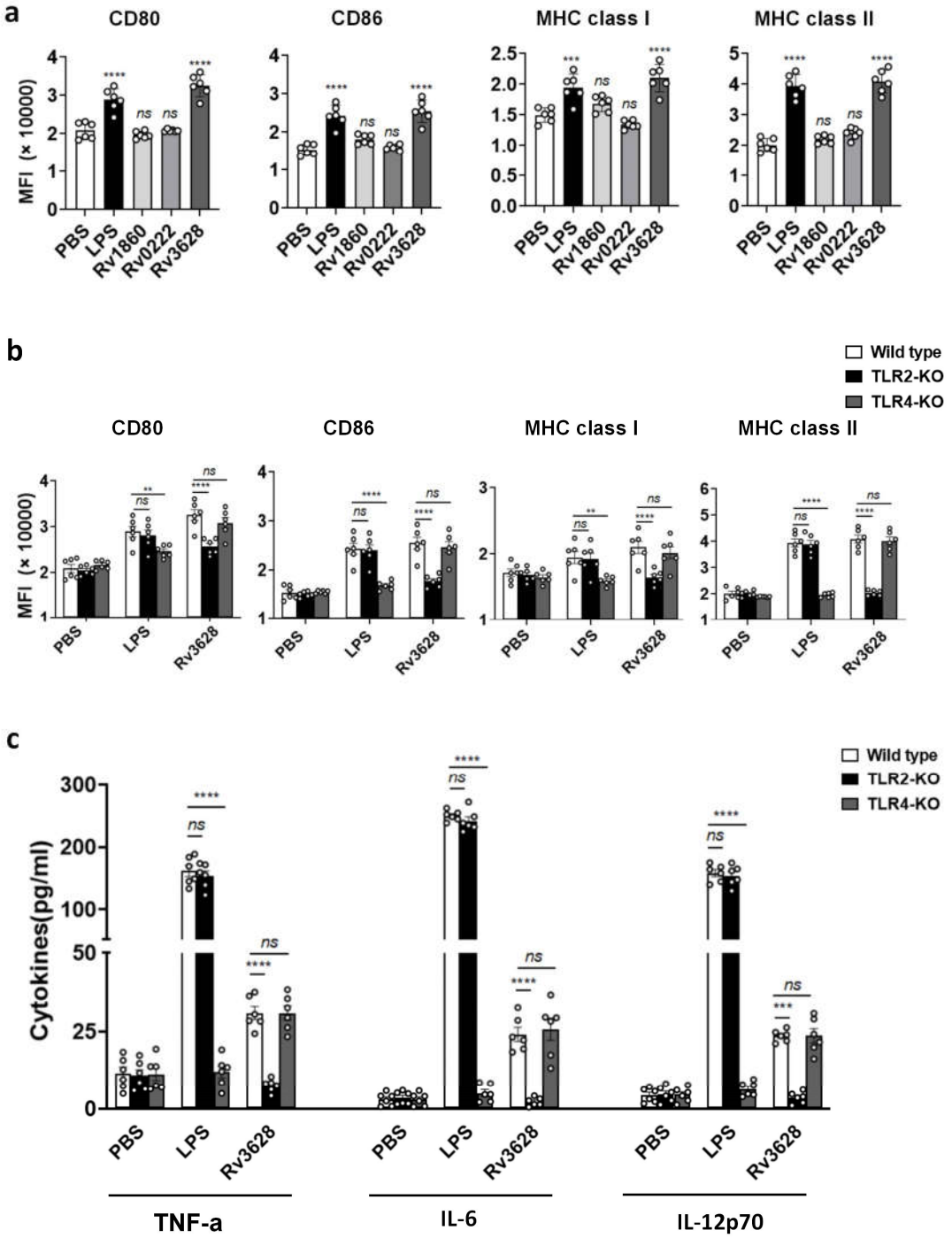

Figure S2. Rv3628 promotes BMDCs activation by interacting with TLR2. BMDCs were treated with 10 μg/mL Rv3628, Rv1860, Rv0222 or with 100 ng/mL LPS for 24 h. (**a)** DCs were stained with anti-CD80, anti-CD86, anti-MHC class I, or anti-MHC class II mAbs and analyzed for the expression of surface markers. The median fluorescence intensity (MFI) of the positive cells is shown. (**b)** and (**c)** DCs derived from WT, TLR2 KO, and TLR4 KO mice were treated with Rv3628 or LPS (100 ng/ml) for 24 h. The bar graphs show the regulation of surface molecules and pro-inflammatory cytokines among $CD11c^{+}$ -gated Rv3628-treated DCs derived from WT, TLR2 KO, and TLR4 KO mice (n = 4 mice, two-way ANOVA, mean ± SEM).

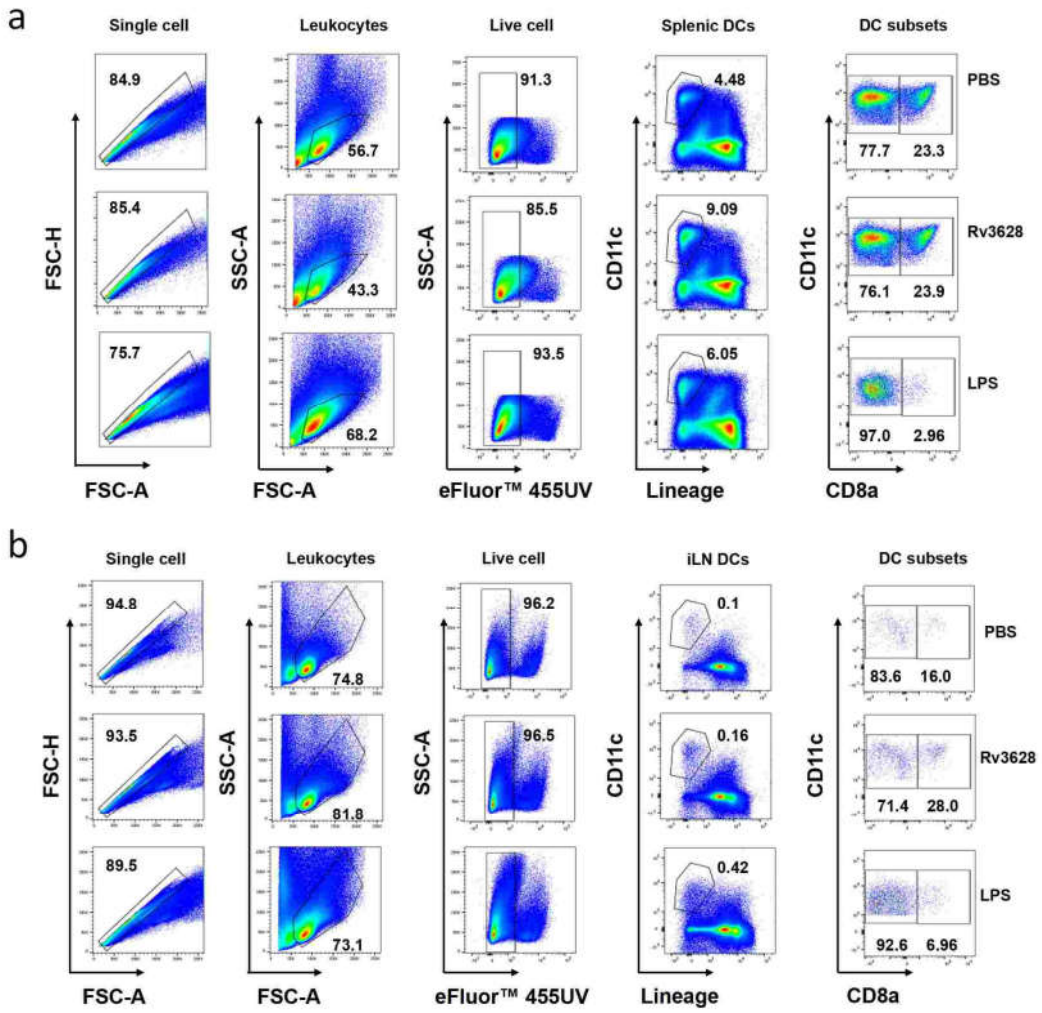

Figure S3. Definition of DCs from spleen and inguinal lymph node (iLN). Spleen and iLN were harvested from C57BL/6 mice and the cells were stained with a lineage marker and CD11c. (**a**) The splenic DCs lineage markers included were anti-B220, anti-CD3, anti-CD49b, anti-Gr1, anti-Thy1.1, anti-TER-119. Lin^- $CD11c^+$ live leukocytes were defined as pDCs. The pDCs were further divided into $CD8\alpha^+$ and $CD8\alpha^-$ DCs. (**b**) The iLN DCs lineage markers included were anti-B220, anti-CD3, anti-CD49b, anti-Gr1, anti-Thy1.1, anti-TER-119. Lin^- $CD11c^+$ live leukocytes were defined as iLN DCs. The iLN DCs were further divided into $CD8\alpha^+$ and $CD8\alpha^-$ DCs.

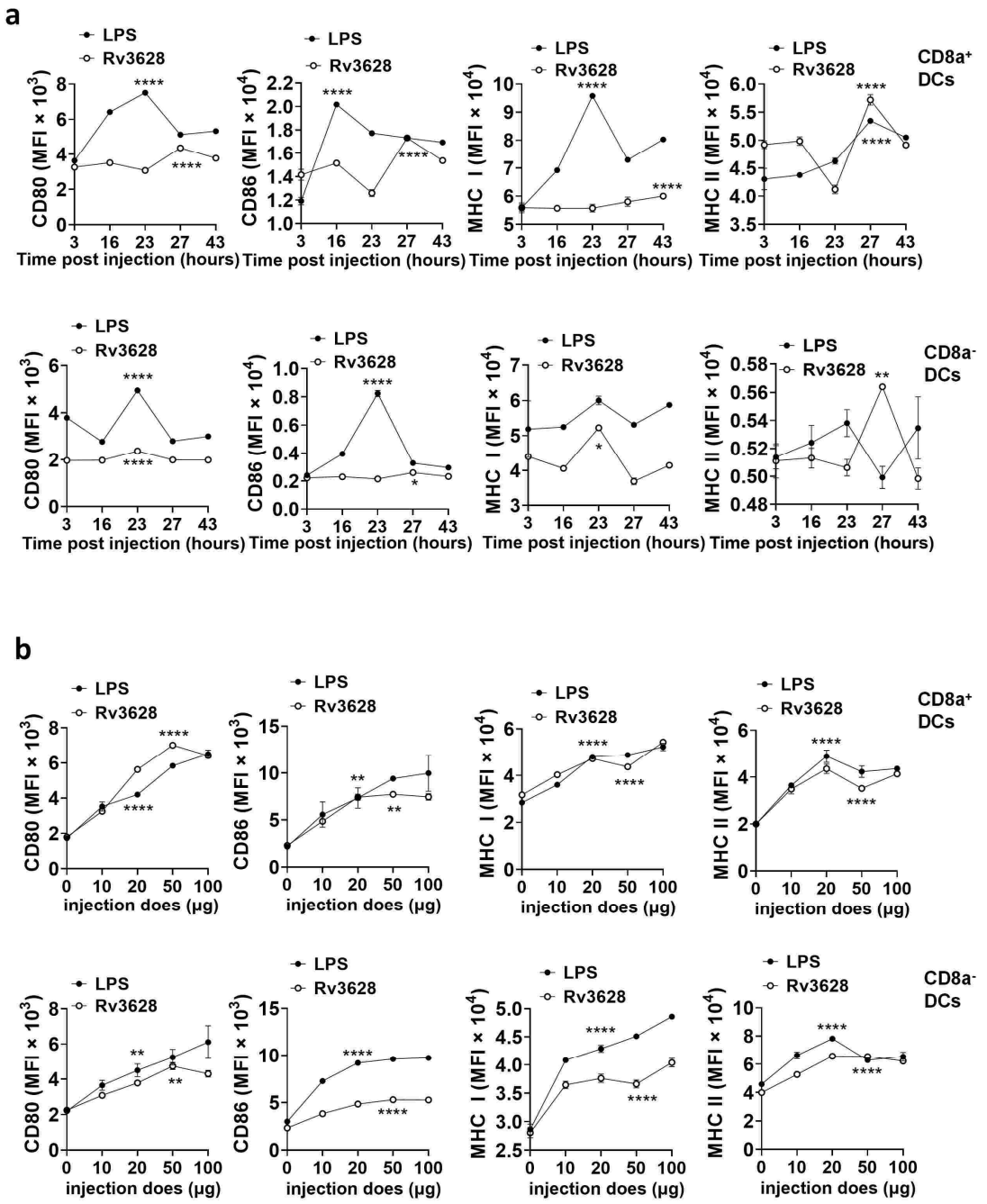

Figure S4. **Dose-dependent and time-dependent effect of Rv3628 on the activation of mouse iLN DCs.** (**a**) C57BL/6 mice were injected i.v. with the indicated dose of Rv3628 or LPS and after 24 h the iLN were harvested. The expression level of co-stimulatory molecules and MHC classes I and II of CD8α$^+$ DCs (upper panel) and CD8α$^-$ DCs (lower panel) are shown. (n = 3 mice, two-way ANOVA, mean ± SEM). (**b**) C57BL/6 mice were injected i.v. with 2.5 mg/kg Rv3628 or 1.0 mg/kg LPS and iLN were harvested as indicated by the time points post-injection. The expression level of co-stimulatory molecules and MHC classes I and II in CD8α$^+$ DCs (upper panel) and CD8α$^-$ DCs (lower panel) are shown. (n = 3 mice,

two-way ANOVA, mean ± SEM).

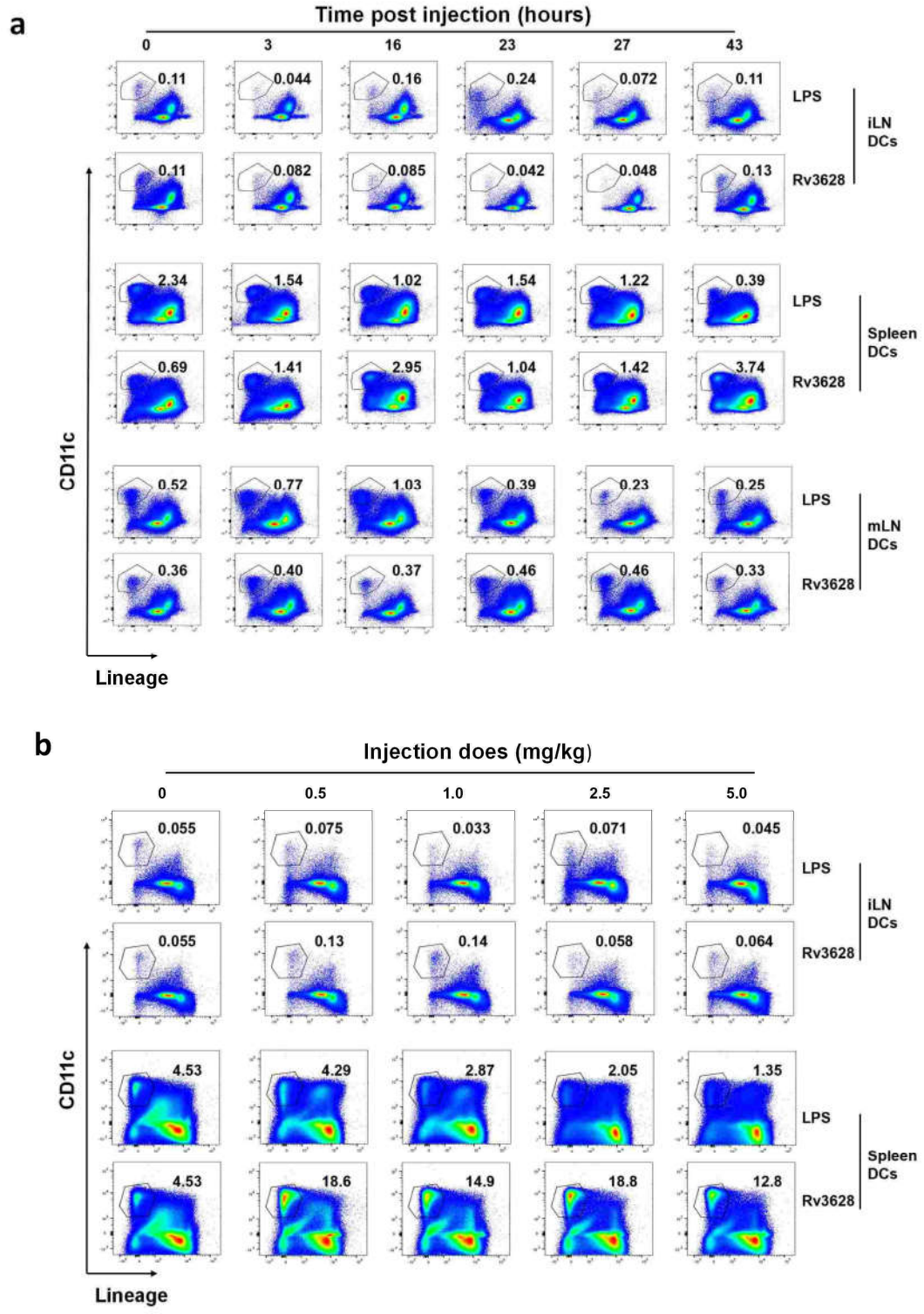

Figure S5. Flow cytometry analysis of dose-dependent and time-dependent effects of Rv3628 on DCs. Representative graphs showing the gating strategy and analysis of DCs. (**a**) C57BL/6 mice were injected *i.v.* with 2.5 mg/kg Rv3628 and 1.0 mg/kg LPS; LN and spleens were harvested at the indicated time points post-injection. (**b**) C57BL/6mice were injected i.v. with the indicated dose of Rv3628 or LPS and 24

h later the iLN, spleen, mLN were harvested.

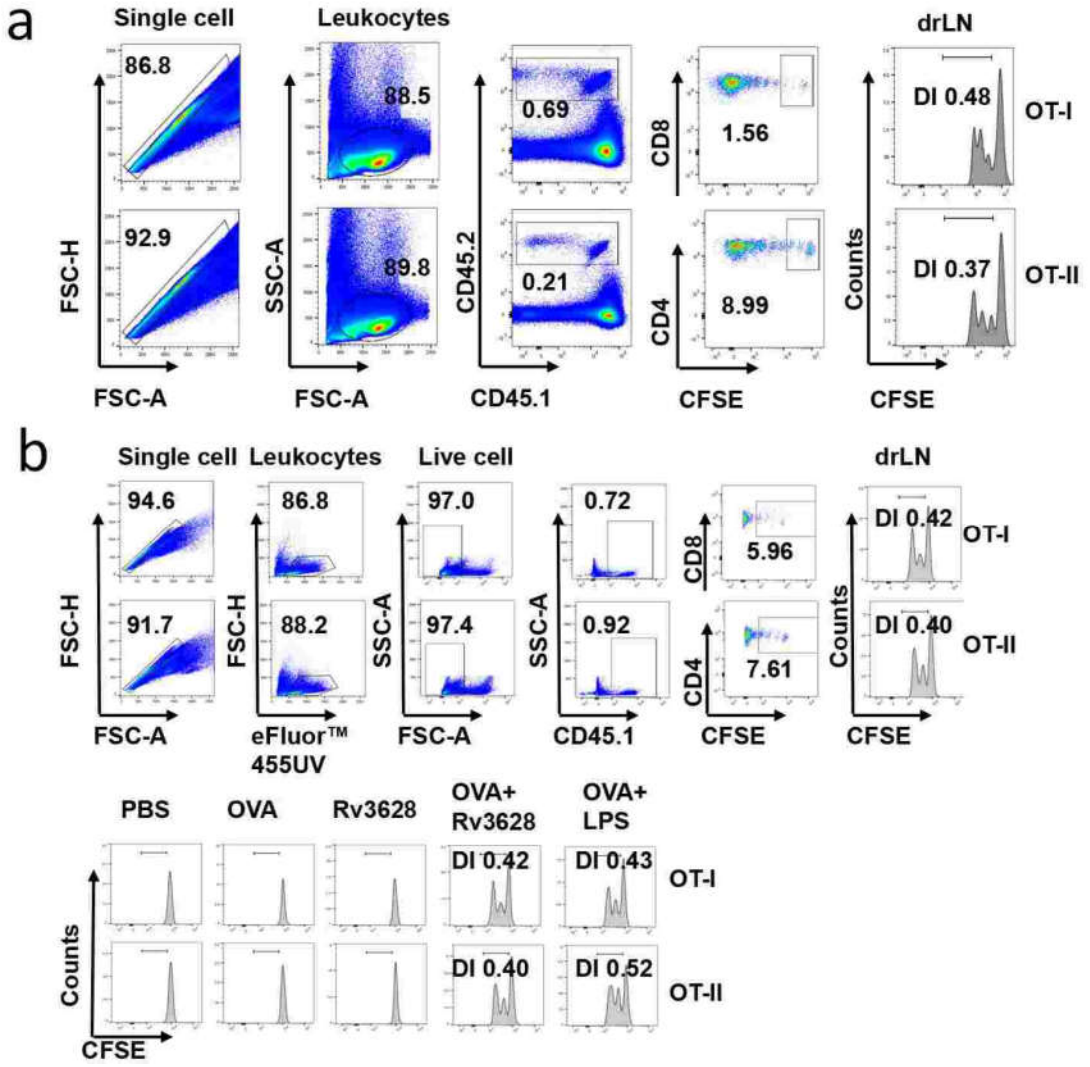

Figure S6. Flow cytometry analysis of OT-I and OT-II cells in iLN. (**a**) The analysis strategy of flow cytometry for detection of CD45.2-expressing OT-I and OT-II cells in iLN from CD45.1 congenic mice and (**b**) from CD45.2 congenic mice.

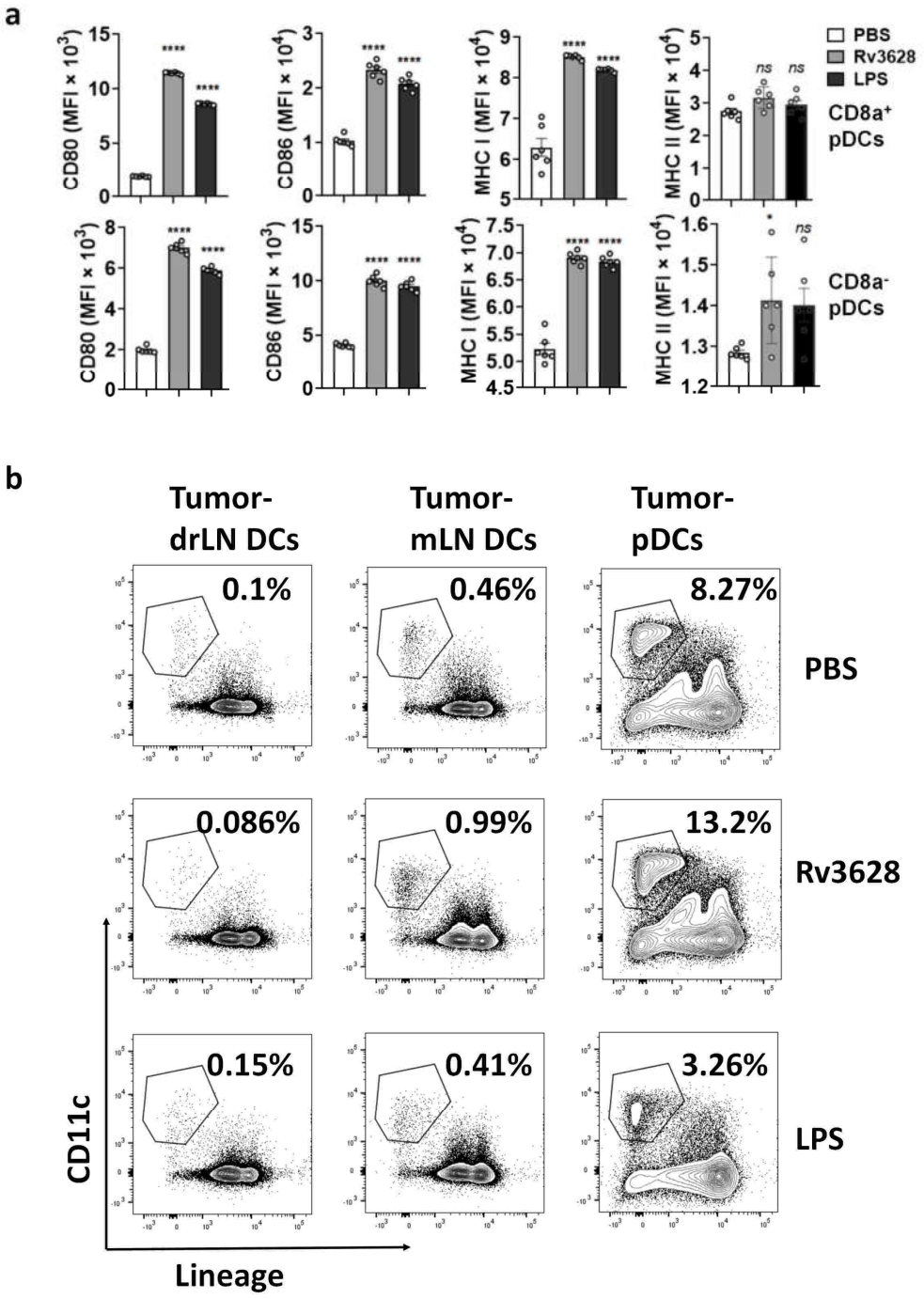

Figure S7. Rv3628-promoted pDC maturation in the tumor microenvironment and characterization of the DCs. C57BL/6 mice were injected *s.c.* with 1 × 10^6 B16 melanoma cells. Fifteen days after tumor injection, the mice were treated with PBS, 2.5 mg/kg Rv3628 or 1.0 mg/kg LPS for 24 h, and then the spleens were harvested. (**a**) The expression levels of co-stimulatory molecules and MHC classes I and II in $CD8\alpha^+$ pDCs (upper panel) and $CD8\alpha^-$ pDCs (lower panel) are shown (n = 6 mice, one-way ANOVA, mean ± SEM). (**b**) Tumor drLN, mLN, spleens were harvested from C57BL/6 and the cells were stained as shown in supplemental Fig.**S2**. Lin^- $CD11c^+$ live leukocytes were defined as DCs.

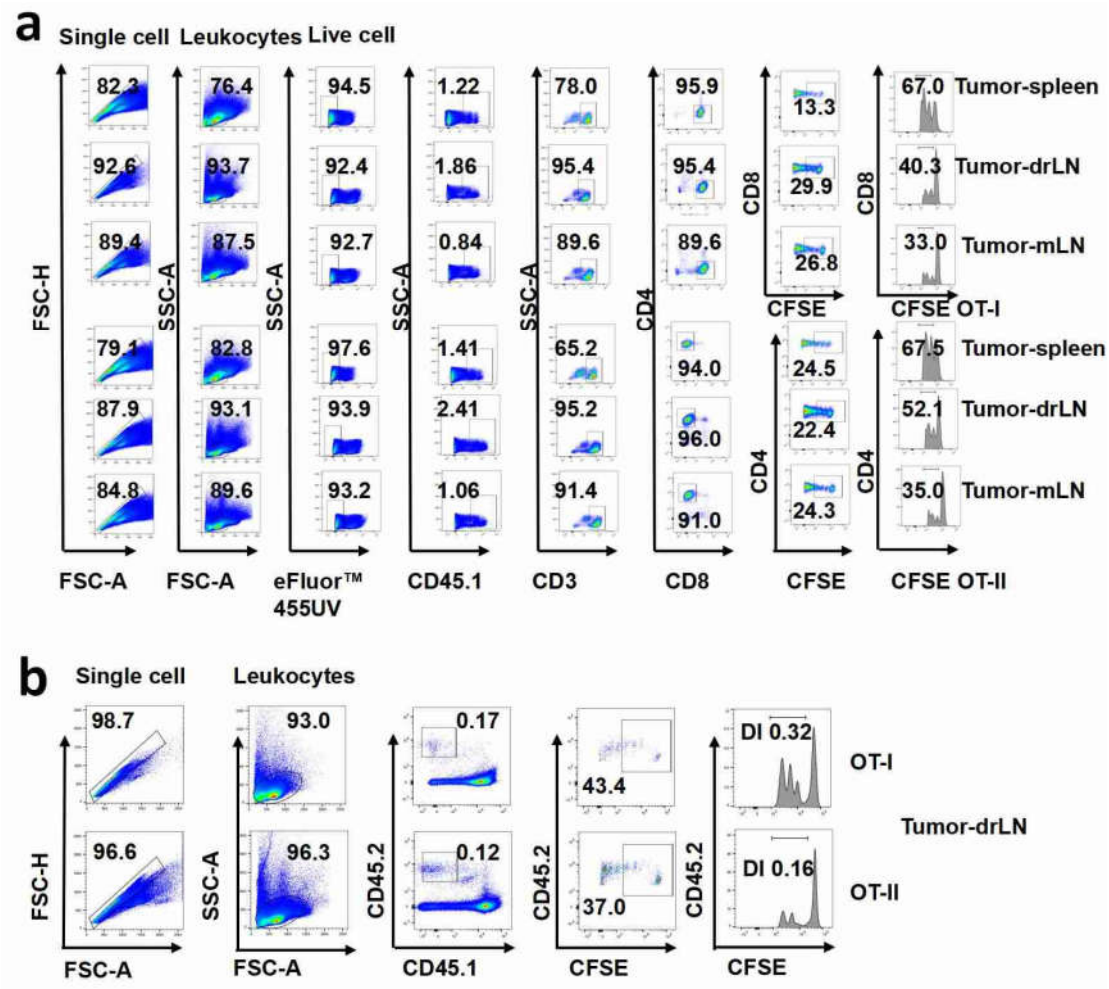

Figure S8. Flow cytometry analysis of OT-I and OT-II cells in mLN and tumor drLN. (**a**) The analysis strategy of flow cytometry for detection of CD45.1-expressing OT-I and OT-II cells in CD45.2 congenic mice. (**b**) Analysis strategy of flow cytometry for detection of CD45.2-expressing OT-I and OT-II cells in CD45.1 congenic mice.

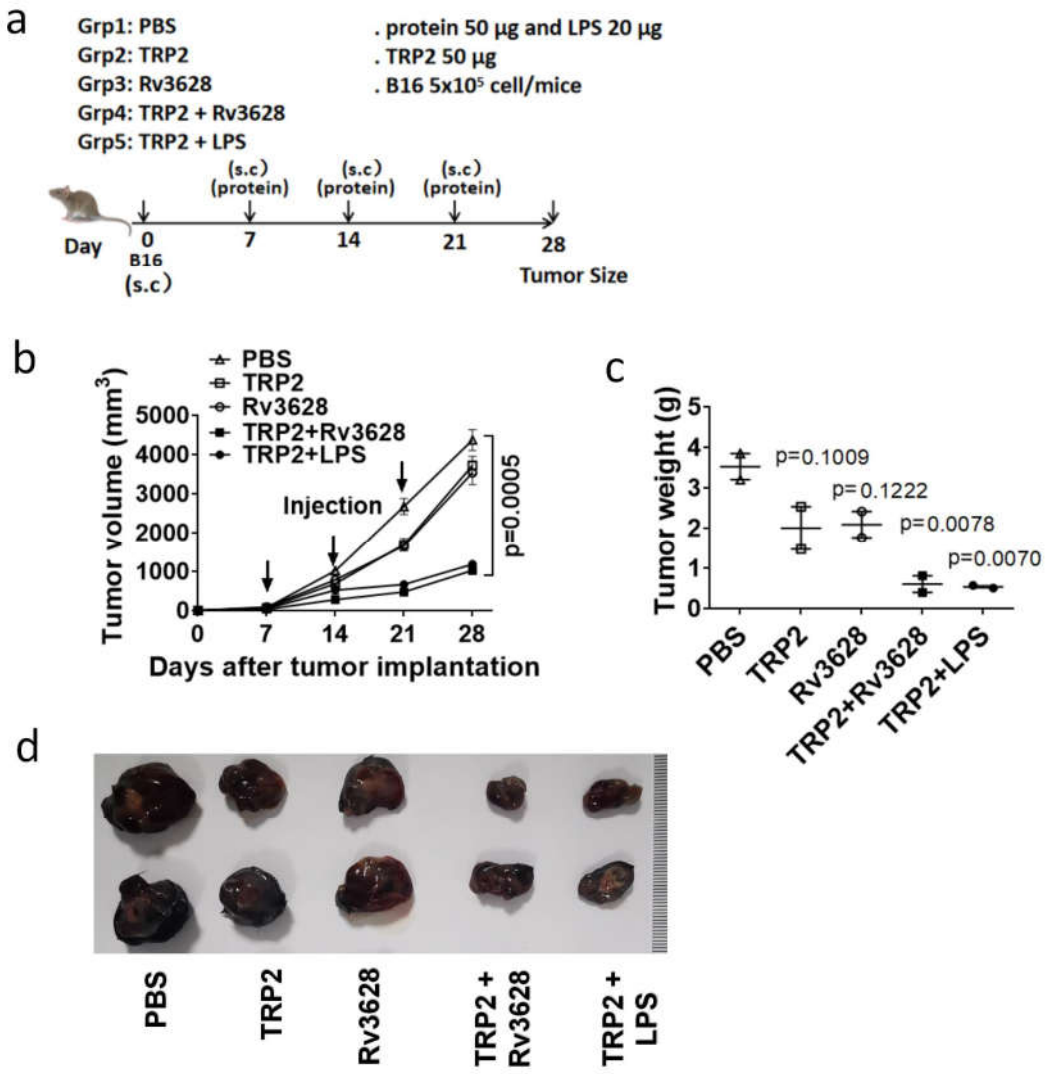

Figure S9. Rv3628 promotes tumor antigen-specific immune activation and immunity against tumor self-Ag TRP2. C57BL/6 mice were injected *s.c.* with 5 × 10^5 B16F10 tumor cells. After 7, 14 and 21 days the mice were treated with PBS or 1.0 mg/kg TRP2, 2.5 mg/kg Rv3628. (**a)** The treatment schedule. (**b)** The curves of B16 tumor growth in mice are shown. (n = 2 mice, two-tailed P value, unpaired t-test, means ± SEM). (**c)** The weights of the tumor masses on day 28 after B16 tumor cell injection. (n = 2 mice, one-way ANOVA, mean ± SEM). (**d)** The size of the tumor masses on day 28 after B16 tumor cell injection. (n = 2 mice).

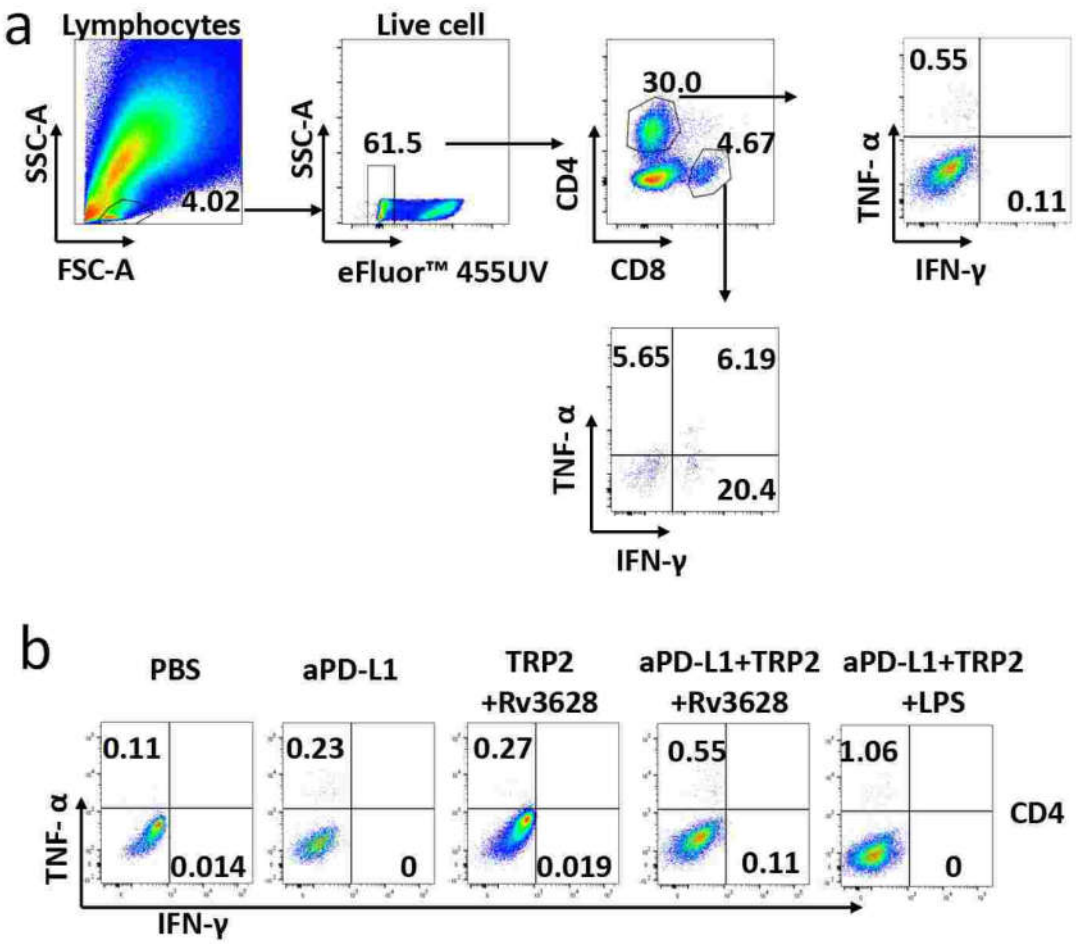

Figure S10. Gating strategy for tumor-infiltrated CTLs present after combination treatment with Rv3628 and anti-PD-L1 antibodies. CTLs in B16 tumors were analyzed by flow cytometry. The strategy of flow cytometry analysis for CTLs in B16 tumors is shown.